PNAS

Main Manuscript for

Correlational selection and genetic architecture shape the evolution of the leaf economics spectrum in a perennial grass

Robert W. Heckman[1,2*], Grace P. John[3], Jason E. Bonnette[1], Brandon E. Campitelli[1,4], Felix B. Fritschi[5], David B. Lowry[6], Philip A. Fay[7], Thomas E. Juenger[1*]

[1] Department of Integrative Biology, University of Texas at Austin, Austin, TX 78712 USA
[2] Current address: U.S. Department of Agriculture Forest Service, Rocky Mountain Research Station, Cedar City, UT 84721 USA
[3] Department of Biology, University of Florida, Gainesville, FL 32611 USA
[4] Current address: McCombs Office of Instructional Innovation, University of Texas at Austin, Austin, TX 78712 USA
[5] Division of Plant Science and Technology, University of Missouri, Columbia, MO 65211 USA
[6] Department of Plant Biology, Michigan State University, East Lansing, MI 48824 USA
[7] U.S. Department of Agriculture Agricultural Research Service, Grassland Soil and Water Research Lab, Temple, TX 76502 USA

* Robert W. Heckman, Thomas E. Juenger

Email: robert.heckman@usda.gov, tjuenger@austin.utexas.edu

Author Contributions: RWH collected data, analyzed data, and led writing with input from TEJ and PAF; TEJ, DBL, and FBF conceived the experiment; GPJ, JEB, and BEC collected data; all authors contributed to writing.

Competing Interest Statement: The authors declare no competing interests

Classification: Biological Sciences, Ecology

Keywords: functional ecology; quantitative genetics; quantitative trait locus; switchgrass; trait-based ecology

This PDF file includes:

Main Text
Figures 1 to 4
Tables 1 to 4

Abstract

The generality of the worldwide leaf economics spectrum (LES) has made it a pillar of trait-based ecological research. Yet, few studies have examined the processes shaping the evolution of the LES within species, in part, because most species occupy only a small portion of the LES. To address this gap, we took advantage of the distinct leaf economics strategies present in different ecotypes of the phenotypically diverse perennial grass *Panicum virgatum* (switchgrass) to generate a genetic mapping population, which we planted in common gardens at three sites spanning 12 degrees of latitude in the central United States. With this genetic mapping population, we evaluated two potentially interacting causes of LES evolution: 1) genetic architecture, where multiple traits are influenced by either the same gene (pleiotropy) or by genes in close physical proximity (genetic linkage), and 2) correlational selection, where selection acts on traits in combination rather than in isolation. We found that shared genetic architecture influenced covariation between photosynthetic rate (A_{MASS}) and leaf nitrogen (N_{MASS}) and between A_{MASS} and leaf mass per area (LMA). We also found that correlational selection favored the trait combinations predicted by the LES (e.g., high LMA with low N_{MASS} or low LMA with high N_{MASS}) and disfavored other, mismatched trait combinations at two of the three sites. Together, these results demonstrate how the evolution of an integrated LES within species can arise from multiple evolutionary causes.

Significance Statement

Understanding how evolution shapes the traits governing plant performance is crucial to predicting species success in a changing world. We studied the genetic links between biomass production, a fitness proxy, and three leaf functional traits that describe a widespread trade-off (leaf mass per area, nitrogen concentration, photosynthetic rate) in a genetic mapping population of switchgrass (*Panicum virgatum*) at sites spanning the central US. Across the genome, three shared loci impacted pairs of leaf functional traits. Additionally, certain combinations of these functional traits were jointly favored by natural selection at two field sites. These findings show that functional strategies in switchgrass can evolve through shared genetic architecture and adaptively favored trait combinations, resulting in integrated phenotypes.

Main Text

Introduction

Globally, plant species exhibit a correlated suite of functional traits known as the worldwide leaf economics spectrum (LES) [1-3]. This spectrum is hypothesized to result from a trade-off between resource acquisition in high resource environments and resource conservation in low resource environments [4]. Evidence for the LES is highly consistent at the global scale [1, 5], leading researchers to incorporate the LES in trait-based studies predicting ecological responses to environmental gradients [6]. However, the LES becomes less consistent at smaller spatial and taxonomic scales [7-9], which may limit the utility of the LES in predicting responses to environmental change at these smaller scales. A critical step toward understanding why the LES sometimes breaks down at smaller scales, and increasing the utility of the LES in predicting the responses of populations and species to environmental change, then, is to identify the evolutionary causes driving integrated leaf economics strategies within species using quantitative genetic tools [4].

The evolution of the LES, like any set of correlated traits, is caused by correlational selection and genetic architecture [10]. Correlational selection favors adaptive trait combinations and disfavors maladaptive combinations, and is likely an important driver shaping functional trait correlations [4]. Correlational selection occurs where selection acts on the covariance between two or more traits and those trait combinations reduce or enhance fitness [11]. By favoring traits in combination rather than in isolation, correlational selection can promote phenotypic integration

[12], potentially explaining the presence of correlated leaf economics strategies. For instance, high photosynthetic rates require leaves with high nitrogen concentrations [1, 4]. Genetic architecture can also constrain or facilitate the evolution of particular trait combinations [13]. Two important ways that genetic architecture can lead to correlated trait evolution are through pleiotropy and genetic linkage. Pleiotropy results when the same gene influences multiple traits. For example, the expression of a gene responsible for the synthesis of chlorophyll, a nitrogen-rich compound, is likely to impact both photosynthetic rate and leaf nitrogen concentration [14]. Genetic linkage results when allelic variation occurs at multiple loci in close physical proximity and those haplotypes are not easily broken apart by recombination [10, 15].

Correlational selection and genetic architecture, which are non-mutually exclusive, can interact to either promote or constrain LES evolution [16]. When correlational selection favors particular trait combinations, but disfavored combinations are genetically linked, evolution of the LES will be constrained [4]. Over generations of recombination, though, selection can break down genetic linkage between these disfavored combinations [17]. Correlational selection can also promote the evolution of genetic linkage between traits [12], generating and maintaining the genetic foundation for the LES. When selection and genetic architecture simultaneously favor the same trait combinations, LES evolution can proceed more rapidly [4]. Thus, understanding how integrated adaptive syndromes like the LES evolve requires accounting for both correlational selection and genetic architecture.

An under-explored means by which resource availability may shape leaf economics strategies within species is variation in growing season length [18]. Specifically, short growing seasons, such as at high latitude or high elevation, may promote an acquisitive strategy of short-lived leaves with low construction costs and high photosynthetic capacity and nutrient concentrations because growth and reproduction are constrained to a narrow window of suitable conditions each year. Long growing seasons, on the other hand, may favor a conservative strategy of long-lived leaves with high construction costs and low photosynthetic capacity and nutrient concentrations [19-21]. For instance, acquisitive strategies in *Populus fremontii* and *Helianthus* spp. were associated with cooler, temperate environments [20, 21].

Disentangling the genetic and environmental components of the LES is key for assessing the potential for LES evolution [4], yet this is difficult to do under the natural field conditions where leaf economics traits are typically measured [1, 22-24]. In this study, we assessed LES evolution by measuring three leaf economics traits—leaf mass per area (LMA), leaf nitrogen concentration (N_{MASS}), and photosynthetic rate (A_{MASS})—in a common environment using a genetic mapping population generated through crosses of distinct ecotypes of the geographically widespread grass *Panicum virgatum* L. (switchgrass). Specifically, we produced a four-way outbred mapping population of full-sibling pseudo-F_2 offspring by crossing the southern lowland genotype, AP13, with the northern upland genotype, DAC, and crossing the southern lowland genotype, WBC, with the northern upland genotype, VS16, then crossing the F_1 progeny. The northern upland ecotype, native primarily to areas with short growing seasons, exhibits an acquisitive strategy of short-lived, high-nutrient leaves, while the southern lowland ecotype, native primarily to areas with long growing seasons, exhibits a conservative strategy of long-lived, low-nutrient leaves [14, 25].

To evaluate genetic architecture, we used a well-established genetic mapping technique, quantitative trait locus (QTL) mapping, to test for associations between different regions of the genome and one or more LES traits [26, 27] in a single common garden in central Texas. To assess correlational selection on leaf economics trait combinations and whether selection changes geographically, we leveraged the ability of this crossing design to break up the adaptive trait combinations often observed in natural populations in order to expose potentially novel or uncommon trait combinations to natural selection. We examined the effect of leaf economics traits and trait combinations on plant fitness to assess correlational selection [28, 29] at three sites spanning 12 degrees of latitude in the central United States (SI Appendix, Table S1).

This allowed us to answer five questions: 1) are leaf economics traits under detectable genetic control? 2) do leaf economics traits covary? 3) is there a genetic component to leaf economics trait covariation? 4) do certain combinations of leaf economics traits increase fitness in

the field? 5) does selection on leaf economics traits change across the geographic range of *P. virgatum*?

Results

Are leaf economics traits under detectable genetic control?
The leaf economics traits evaluated here had a substantial genetic basis. In a common garden in central Texas, all three leaf economics traits exhibited moderate broad-sense heritability (H^2; Table 1). Of the three, A_{MASS} had the lowest heritability (H^2 = 0.26), while LMA and N_{MASS} had similar, and higher, heritability (H^2 = 0.51 and 0.46, respectively). For each trait, we detected 4–5 significant QTL (Table 2), which together explained 15–35% of variation (Table 1).

Do leaf economics traits covary phenotypically?
In this system, phenotypic correlations among the pairs of leaf economics traits were statistically significant, although sometimes biologically weak. Among F_2 individuals generated by crossing northern and southern genotypes with distinct leaf economics strategies, significant bivariate relationships existed amongst all pairs of leaf economics traits. Consistent with global LES relationships, LMA covaried negatively with N_{MASS} (R^2 = 0.06, P < 0.001; Fig. 1a) and with A_{MASS} (R^2 = 0.29, P < 0.001; Fig. 1b); N_{MASS} and A_{MASS} covaried positively (R^2 = 0.06, P < 0.001; Fig. 1c).

Is there a genetic component to leaf economics trait covariation?
Covariation between leaf economics traits exhibited some genetic contribution. We detected 13 QTL across the three leaf economics traits, all of which were highly significant predictors of the LES traits in multiple-QTL models (P < 0.05; Table 2). These 13 QTL included three pairs of colocalized QTL (i.e., confidence intervals for the QTL overlapped; Fig. 2a): QTL for LMA and A_{MASS} co-occurred on chromosome 9K and QTL for A_{MASS} and N_{MASS} co-occurred at two locations on chromosome 2K.

We then evaluated whether the genetic architecture of these three pairs of traits can best be explained by the null hypothesis of a single QTL for both traits (i.e., statistical pleiotropy) or by the alternative hypothesis of two separate QTL (genetic linkage) using a bootstrapped multivariate QTL scan [30]. Because we could not reject the null hypothesis that these colocalized QTL were produced by a single QTL (P = 0.14, P = 0.254, and P = 0.429, respectively; Fig. 2b-d), our results for all three pairs of colocalized QTL are more consistent with the hypothesis of statistical pleiotropy than with genetic linkage. Marker regression also showed that genotype effects at colocalized QTL were in the same direction for both traits (i.e., both conservative or both acquisitive), which further supports statistical pleiotropy. Specifically, individuals possessing two upland alleles at the QTL on chromosome 2K had lower A_{MASS} and N_{MASS} than other genotypes (Chr2K@11.9 and Chr2K@10.3, respectively; Fig. 2b). Similarly, individuals with two upland alleles at the QTL on chromosome 9K had significantly higher A_{MASS} and significantly lower LMA than other genotypes (Chr9K@13.3 and Chr9K@12.4, respectively; Fig. 2d).

Although we detected colocalized QTL for some trait pairs, genetic correlations—the proportion of genetic variance across the entire genome shared between traits—were inconsistent. We found a significant genetic correlation between LMA and A_{MASS} (r_g = -0.75, χ^2 = 15.87, P < 0.001; Table 3), but not between LMA and N_{MASS} (r_g = -0.16, χ^2 = 0.80, P = 0.37) or between A_{MASS} and N_{MASS} (r_g = 0.24, χ^2 = 1.11, P = 0.29). These contrasting effects may be related to the directionality of QTL inherited from parents and grandparents of different ecotypes for the three LES traits. Based on marker regression, all five significant QTL for LMA were in the same direction, which was consistent with a conservative leaf economics strategy among the lowland ecotype and an acquisitive strategy among the upland ecotype (i.e., individuals with both lowland alleles had high LMA and individuals with both upland alleles had low LMA; Fig. 2d; SI Appendix, Fig. S1a–d). Conversely, some QTL for A_{MASS} and N_{MASS} behaved opposite to LES predictions—at these QTL, individuals with both upland alleles had low N_{MASS} and low A_{MASS},

while individuals with both lowland alleles had high N_{MASS} and high A_{MASS} (A_{MASS}: Chr2K@11.9 and Chr2K@59.8, N_{MASS}: Chr2K@10.3, Chr2K@61.8, and Chr5K@21.5, respectively; Fig. 2b–c; SI Appendix Fig., S1e–g). When QTL differ in direction, as QTL for LMA and N_{MASS} sometimes differed from one another, it may weaken the aggregate genetic correlations between the two traits [31]. Similarly, despite detecting two colocalized QTL for A_{MASS} and N_{MASS}, these pairs of colocalized QTL were in the opposite direction of typical leaf economics strategies, which could also weaken genetic correlations.

Do certain combinations of leaf economics traits increase fitness in the field?
Using aboveground biomass measured on clonally propagated individuals at three common gardens spanning 12 degrees of latitude (SI Appendix, Table S1), genetic selection gradient analysis revealed that correlational selection may promote leaf economics trait covariation. Consistent with our hypothesis, LMA and N_{MASS} interacted significantly to impact biomass production averaged for each F_2 genotype across the three sites [32]: genotypes expressing acquisitive trait combinations (i.e., high N_{MASS} and low LMA) or conservative trait combinations (low N_{MASS} and high LMA) produced more biomass than plants with mismatched combinations of N_{MASS} and LMA (γ_{ij} = -0.037, P = 0.027; Table 4A; SI Appendix, Table S2; Fig. 3).

Does selection on leaf economics traits change across the geographic range of P. virgatum?
Selection on leaf economics traits varied geographically, favoring a conservative strategy in the south, where growing seasons are long, and an acquisitive strategy in the north, where growing seasons are short. In site-specific phenotypic selection gradients, directional selection at the southern site (Austin, TX) favored a conservative, low N_{MASS} strategy (β = -0.081, P < 0.001; Table 4B; SI Appendix, Table S3; Fig. 4A), but there was no significant correlational selection (γ_{ij} = - 0.001, P = 0.949). At our mid-latitude site (Columbia, MO), directional selection favored a conservative, high LMA strategy (β = 0.070, P = 0.005), while correlational selection also favored individuals possessing conservative values of both traits (i.e., high LMA, low N_{MASS}) or acquisitive values of both traits (i.e., low LMA, high N_{MASS}) over individuals with mismatched trait combinations (high LMA and high N_{MASS} or low LMA and low N_{MASS}) (γ_{ij} = -0.043, P = 0.099; Table 4C; SI Appendix, Table S3; Fig. 4B). At the northern site (Hickory Corners, MI), directional selection favored an acquisitive, low LMA strategy (β = -0.038, P = 0.083). There were also quadratic effects of LMA and N_{MASS} on biomass that were concave down (LMA: γ = -0.059, P = 0.031; N_{MASS}, γ = -0.043, P = 0.091) and interactive effects of LMA and N_{MASS} on biomass production, indicating correlational selection favoring the acquisitive strategy of high N_{MASS} and low LMA (γ_{ij} = -0.051, P = 0.034; Table 4D; SI Appendix, Table S3; Fig. 4C). Critically, the general agreement between these phenotypic selection gradients and the genetic selection gradients described above indicates that environmental covariances between traits and fitness were not the primary drivers of these results [32].

Discussion

Identifying the evolutionary causes of leaf economics strategies is critical for understanding the scales at which the LES operates, yet few studies have explored this [4]. Studies of LES evolution within species are relatively rare, in part, because past evolution has eliminated considerable variation from most populations, leaving most species, and even many genera, to occupy a small portion of the LES [9, 33] [but see 4]. But species possessing distinct ecotypes or occupying a broad range of habitats may harbor sufficient variation for us to evaluate microevolution of the LES. Thus, species like *P. virgatum*, where distinct leaf economic strategies exist [14, 25], provide a unique opportunity to create combinations of traits not observed in natural populations and examine whether selection changes across the species' range. Here, we show strong evidence for LES evolution within *P. virgatum*: genetic architecture, and correlational selection that differed among sites, generally promote the hypothesized leaf economics strategies, but some genetic constraints may limit LES evolution in this system [34].

Our results also demonstrate an important role for genetic architecture in structuring the LES within *P. virgatum*. At individual QTL, we found evidence that genetic architecture could explain leaf economics trait covariation. Specifically, we found evidence consistent with statistical pleiotropy among QTL controlling both N_{MASS}–A_{MASS} and A_{MASS}–LMA, which aligns with more recent work showing that pleiotropic QTL control some leaf economics trait correlations in *Arabidopsis thaliana* [35, 36]. Yet this did not always translate into consistent genetic correlations between pairs of leaf economics traits. In fact, only A_{MASS} and LMA exhibited a significant genetic correlation. These inconsistent genetic correlations, which aggregate the effects of many QTL across the genome, may have resulted from differences in the QTL inherited from upland and lowland parents and grandparents across different leaf economics traits. All five putative QTL for LMA exhibited divergence in the same direction—plants with lowland alleles exhibited higher LMA than plants with upland alleles—which is consistent with a conservative strategy among the lowland ecotype and an acquisitive strategy among the upland ecotype of *P. virgatum* [37]. In contrast, QTL for A_{MASS} and N_{MASS} did not show consistent QTL directionality—the acquisitive strategy of high A_{MASS} and N_{MASS} was associated with lowland or upland alleles at different QTL. Deviations in genetic architecture from what is predicted by the LES, especially the lack of a genetic correlation between LMA and N_{MASS}, may be explained by differences in selection across the range of *P. virgatum*, either spatially or temporally [18].

In this study, selection on leaf economics traits favored matched combinations of LMA and N_{MASS} at the genetic level. Phenotypically, selection favored different strategies across the range of the species: a conservative strategy typical of the southern lowland ecotype was favored at our southern site, while an acquisitive strategy typical of the northern upland ecotype was favored at our northern site. The general concordance between these genetic and phenotypic selection gradients—that correlational selection is often significant—reinforce the overall finding and suggest that these results were not primarily driven by environmental covariances between leaf economics traits and fitness [32]. The shift in phenotypic selection across the range of *P. virgatum* may have been driven by differences in growing season length across the species' range [18], which is consistent with previous work in *A. thaliana*, *Populus* spp., and *Helianthus* spp. showing that long growing seasons favor a conservative leaf economics strategy and short growing seasons favor an acquisitive strategy [20, 21, 38]. While growing season length is not the only potential driver that varied among our sites, these results are consistent with recent work in *P. virgatum* showing that leaf strength—a key factor promoting long-lived, high LMA leaves (i.e., a conservative strategy)—increased with the growing season length from which genotypes originated [39]. Future studies could examine whether growing-season length is as important a driver of LES evolution as resource availability, an oft-hypothesized driver of the LES [1, 3], by evaluating the fitness of conservative and acquisitive genotypes under experimentally manipulated resource supply along a latitudinal gradient.

Conclusions

Here, we use a tractable system to show that the LES can evolve through a combination of genetic architecture and correlational selection favoring individuals possessing certain combinations of LMA and N_{MASS}, which changed across the species' geographic range. It is unclear, however, whether evolution of the LES in *P. virgatum* is driven by the same resource-driven trade-off between resource acquisition and conservation that is hypothesized to underlie the worldwide LES [1, 3]. Nonetheless, quantifying the importance of these processes to the evolution of the LES within species may help resolve inconsistencies seen in LES studies performed at different scales and further our understanding and prediction of evolutionary responses to environmental change.

Materials and Methods

Study system

Panicum virgatum is an ecologically and economically important species possessing large phenotypic variation in leaf economics traits [25, 40, 41]. It is common throughout central North

American grasslands, occupying habitats that vary considerably in season length and mean annual temperature and precipitation [42]. To occupy these diverse habitats, *P. virgatum* has diverged into three ecotypes—upland, coastal, and lowland—with the coastal ecotype exhibiting characteristics intermediate between the other two [43]. The upland ecotype typically occurs in northern regions with short growing seasons and possesses an acquisitive strategy of high-nutrient leaves with high photosynthetic rates and low LMA. The lowland ecotype occurs in southern regions with long growing seasons and possesses a conservative strategy of low-nutrient leaves with low photosynthetic rates and high LMA [14, 25, 40, 44].

Experimental setup

In this study, we addressed the first three research questions—whether leaf economics traits are under detectable genetic control; whether leaf economics traits covary; and whether there is a genetic component to leaf economics trait covariation—with plants grown at a single site. We addressed the fourth and fifth research question—whether certain combinations of leaf economics traits increase fitness in the field; and whether selection changes geographically—by replicating the design of the single-site study at three sites spanning a broad latitudinal gradient in the central United States.

This experimental design is described in detail by Milano et al [37] and Lowry et al [45]. In summary, a genetic mapping population was developed by crossing the southern lowland genotype, AP13 (Alamo) with the northern upland genotype, DAC (Dacotah) and by crossing the southern lowland genotype, WBC (West Bee Cave) with the northern upland genotype, VS16 (Summer). Single F_1 offspring from each of these two crosses were then reciprocally crossed to produce a four-way outbred mapping population, which contained ~700 full-sibling pseudo-F_2 offspring, half of which arose from each direction of cross (i.e., which F_1 offspring was the pollen donor), resulting in a design that balanced inheritance of cytoplasm (including chloroplasts) from the upland and lowland ecotypes across F_2 individuals. By recombining upland and lowland alleles, this cross generated F_2 individuals that carry either two lowland alleles, two upland alleles, or one lowland and one upland allele at each locus. The F_2 offspring were then clonally propagated in 3.8-L pots at Brackenridge Field Laboratory, University of Texas at Austin, Austin, TX.

For the single-site portion of this study, individuals of ~400 unreplicated F_2 genotypes were transplanted into a common garden at Brackenridge Field Laboratory in February 2014 [37]. The field was first covered with landscape fabric (Sunbelt 3.2 oz, DeWitt, Sikeston, MO, USA) and individuals were planted into holes cut in the fabric. Plants were randomly assigned to locations in the field in a honeycomb design, with each plant located 1.25 m from its four nearest neighbors. To prevent edge effects, the field was surrounded with a border row of plants of the lowland genotype AP13.

For the multi-site portion of this study, clonally propagated individuals of ~700 F_2 genotypes, including the 400 F_2 genotypes used in the single-site portion of the study, were planted in spring 2015 at three locations throughout the central United States (Pickle Research Campus, University of Texas at Austin, Austin, TX, USA; Bradford Research Center, University of Missouri, Columbia, MO, USA; Kellogg Biological Station, Michigan State University, Hickory Corners, MI, USA) that spanned 12 degrees of latitude [45]. Plantings at these three sites were identical in layout to the single-site planting described in the previous paragraph [see 45 for details].

Leaf economics measurements

In the single-site portion of this study, we measured three leaf economics traits— leaf mass per area (LMA), mass-based leaf nitrogen concentration (N_{MASS}), and mass-based photosynthetic capacity (A_{MASS})—on 1–7 July 2014. To calculate LMA, we measured the area of one penultimate, fully expanded sun leaf per plant using a portable leaf area meter (LI-3000C, LI-COR Biosciences, Lincoln, NE, USA), then dried each leaf at 65 °C to constant mass and weighed it. LMA is the ratio of leaf dry mass to leaf area. To calculate N_{MASS}, each dried leaf was ground to a fine powder with 4 mm steel beads in a tissue homogenizer (SPEX GenoGrinder 2000, SPEX

SamplePrep, Metuchen, NJ, USA), then combusted in an elemental analyzer (Flash 2000 Organic Elemental NC Analyzer, Thermo Scientific, Waltham, MA, USA). To measure photosynthetic capacity, we enclosed two penultimate, fully expanded sun leaves in the 2-cm × 3-cm cuvette of a portable photosynthesis system (LI-6400XT, LI-COR Biosciences, Lincoln, NE, USA) between 10:30 and 14:00 on sunny days. To reduce the likelihood of spurious results, we haphazardly chose the order and direction in which rows of plants were surveyed in the field. Photosynthetically active photon flux density was maintained within the cuvette at 1750 μmol m^{-2} s^{-1} using an actinic light source. Because ambient light availability during the measurement period was comparable to, or exceeded, light in the cuvette, we did not consider a threshold level of ambient light level prior to taking measurements. Chamber CO_2 supply was set to 400 ppm, and leaf temperature and water vapor content of incoming air were allowed to track ambient conditions. Following [25, 46], we logged measurements after fluxes of CO_2 and H_2O stabilized, usually within 3–4 minutes of clamping onto a leaf, rather than enforcing a minimum chamber acclimation period for the leaves. We converted from an area-basis (A_{AREA}) to a mass-basis (A_{MASS}) by dividing A_{AREA} by LMA.

In the multi-site portion of this study, we measured LMA and N_{MASS} on May 25, 2018 in Austin, TX, on August 2, 2018 in Columbia, MO, and on August 5, 2018 in Hickory Corners, MI, on ~300–350 F_2 individuals per site. We slightly modified the field sampling approach described above to measure N_{MASS}. Specifically, N_{MASS} was measured by collecting and drying five recently expanded sun leaves, then grinding them with 8-mm and 4-mm steel beads in a different tissue homogenizer (SPEX GenoGrinder 2010, SPEX SamplePrep, Metuchen, NJ, USA) and combusting the samples in a different elemental analyzer (CN 802, Velp Scientifica, Deer Park, NY, USA).

Fitness measurements

In the multi-site portion of this study, we quantified aboveground biomass production as a proxy for fitness. It is difficult to know the appropriate fitness measure for a long-lived perennial that can spread clonally through vegetative reproduction and through seed [47, 48], but our use of this fitness proxy is supported by a few lines of evidence. First, previous work has found that aboveground biomass is highly correlated with seed production in *P. virgatum* [49], making it a useful proxy for reproductive fitness [45]. Second, a recent meta-analysis demonstrated that plant functional traits exhibited similar degrees of selection via performance (i.e., biomass production) and fitness (i.e., survival, reproduction) [50].

In November 2018, we first harvested plants at ~15 cm above ground level and weighed their fresh mass with a hanging scale (OP-926, Optima Scale Inc., Rancho Cucamonga, CA, USA). We then weighed a representative subsample of each plant before and after drying at 65 °C to determine percent moisture of the subsample. Finally, we converted fresh mass to dry mass by multiplying the percent moisture of the subsample by the fresh mass of the entire plant.

Quantitative genetic and other statistical analyses

To assess whether leaf traits in *P. virgatum* form a leaf economics spectrum, we fit standardized major axis (SMA) regression models for each pair of leaf traits measured in the single-site common garden [sma() function in package smatr, 51]. SMA regression is commonly used in functional ecology because, unlike least squares regression, it assumes that both variables are measured with error [52]. As described by [1], the LES is represented by a significant positive relationship between A_{MASS} and N_{MASS} and negative relationships between LMA and A_{MASS} and between LMA and N_{MASS}.

To quantify the degree of genetic control of leaf economics traits, we calculated broad-sense heritability (H^2) of leaf economics traits measured in the single-site common garden by fitting a linear mixed model that accounted for the relatedness among individuals with an additive genetic relatedness matrix [i.e., animal model; mmer() function, package sommer, 53, 54]. Broad-sense heritability was calculated as the ratio of variance among lines (genetic variance, V_G) to total variance (V_G + environmental variance, V_E) in each trait (V_G / V_G + V_E). Throughout, we refer

to V_G and H^2 rather than additive genetic variance (V_A) and narrow-sense heritability (h^2) because additive and dominance genetic variance are confounded in this full-sib cross [55].

To estimate the proportion of variance shared among leaf traits due to genetic causes (genetic correlations, r_g), we fit a multivariate extension of the linear mixed model described in the previous paragraph, which included all three leaf economics traits as responses. Genetic correlation was the ratio of the genetic covariance between each pair of traits (COV_G) to the square root of the products of their genetic variances, $r_g = \mathrm{Cov}_G / \sqrt{V_{G1} \times V_{G2}}$. To estimate the significance of these genetic correlations, we compared a model in which the genetic covariance between a pair of traits was estimated freely to a model in which the genetic covariance between those traits was constrained to 0 (i.e., no genetic covariance between traits was allowed) with a likelihood ratio test. A significant likelihood ratio test indicates that genetic covariance differs from 0.

QTL mapping

We conducted QTL mapping on leaf economics traits in the single-site common garden [package qtl2, 56]. Methods for constructing the linkage map used in this analysis are described by [57]. First, we assessed the likelihood that each genetic marker is associated with a phenotype of interest by performing a genome scan with a leave-one-chromosome-out kinship matrix [scan1() function]. This provided log-odds (LOD) scores for every marker in the genome. From these LOD profiles, we identified putative QTL at a significance threshold of α = 0.15 [find_peak() function with drop = 1.5 and peakdrop = 2.5]. We determined the LOD score corresponding to this significance threshold via permutation test with 1000 iterations [scan1perm() function]. We chose a relaxed significance threshold because a stricter threshold could hinder a primary goal of this study—to detect and evaluate QTL overlap among leaf traits. To maintain statistical rigor when evaluating putative QTL, we further assessed the significance and explanatory power of all QTL by fitting a multiple-QTL model for each phenotype [makeqtl() and fitqtl() functions in package qtl, 58]. This multiple-QTL model detected significant effects of all putative QTL identified by the initial genome scan ($P < 0.05$).

When QTL confidence intervals for two traits overlapped, we tested the hypothesis that this overlap was due to statistical pleiotropy (one QTL) or separate QTL using a pipeline from the qtl2pleio package [30]. To do this, we first identified the region of QTL overlap [scan_pvl() function], then identified the marker corresponding to the peak of the pleiotropy trace [find_pleio_peak_tib() function], then performed a bootstrapped multivariate QTL scan with 1000 iterations [boot_pvl() function] to evaluate the evidence for separate QTL. In this analysis, the null hypothesis is one QTL (i.e., statistical pleiotropy). Thus, $P > 0.05$ indicates a lack of evidence for separate QTL and is more consistent with the statistical pleiotropy hypothesis than with the genetic linkage hypothesis.

Selection gradient analysis

To assess linear and non-linear selection on leaf economics traits at multiple field sites, we fit both genetic and phenotypic selection gradients. We assessed both types of selection gradients by fitting a generalized least squares model [gls() function in package nlme, 59] in which LMA and N_{MASS} were predictors of aboveground biomass production. Each model included main effects (i.e., linear directional selection) and doubled quadratic effects (i.e., non-linear stabilizing or disruptive selection) of each trait [60] and the two-way interaction between the traits (i.e., non-linear correlational selection). The genetic selection gradient model allowed us to assess overall selection while reducing confounding environmental effects [32] by fitting the model to genotype-level means of biomass, LMA, and N_{MASS} calculated across the three sites. The phenotypic selection gradient models allowed us to assess changes in selection across a latitudinal gradient by fitting separate models for each site using site-specific values of biomass, LMA, and N_{MASS}. Prior to analysis, aboveground plant biomass (our fitness proxy) was mean-standardized by dividing the biomass of each genotype or plant by mean biomass, resulting in a relativized proxy for fitness, such that average fitness is equal to 1; above average fitness > 1; and below average fitness < 1 [11, 48, 60], and LMA and N_{MASS} were mean-centered and variance-standardized

(mean = 0, standard deviation = 1). For phenotypic selection gradients, biomass, LMA, and N_{MASS} were standardized within sites. These two types of selection gradient models are complementary to one another. Genetic selection gradients isolate genetic effects from environmental effects, which helps to overcome one of the limitations of phenotypic selection gradients—that environmental covariances between traits and fitness can bias estimates of phenotypic selection [32]. Moreover, genetic selection gradients assess the strength of genetic links between traits and fitness, which is necessary for evolution by natural selection to proceed [10]. Here, phenotypic selection gradients provide information about how selection can occur within distinct sites with diverse climates, where our experimental design precludes the use of genetic selection gradients. Results that agree across these analyses reinforce one another and provide stronger support for the type of selection observed [32].

Data, Materials, and Software Availability

The dataset and code used in this study have been deposited in figshare (https://doi.org/10.6084/m9.figshare.17215103).

Acknowledgments

We thank Quinn Hiers and Albina Khasanova for help with data collection. Elizabeth Alger, Tina Arredondo, Nicole Carrabba, Elena Pinaroc, Maya Rao, Maria Villalpando, Lisa Vormwald, and Heather Yang also provided field assistance. We're grateful to Natasha Pagel-Aprill, Tim Fegel, Isabel McPherson, and Chuck Rhoades for performing leaf N analyses. Alice MacQueen and other members of the Juenger lab provided helpful comments on a previous draft of the manuscript. This work was supported by NSF PGRP IOS 0922457 and IOS 1444533. This research was supported by the Office of Science (BER), U.S. Department of Energy, Grant no. DE-SC0014156 and in part by the U.S. Department of Agriculture Forest Service, Rocky Mountain Research Station. This material is based upon work supported by the Great Lakes Bioenergy Research Center, U.S. Department of Energy, Office of Science, Biological and Environmental Research Program under Award Number DE-SC0018409. The findings and conclusions of this publication are those of the authors and should not be construed to represent any official USDA or U.S. Government determination or policy.

References

1. Wright, I.J., et al., *The worldwide leaf economics spectrum.* Nature, 2004. **428**(6985): p. 821-827.
2. Shipley, B., et al., *Fundamental trade-offs generating the worldwide leaf economics spectrum.* Ecology, 2006. **87**(3): p. 535-541.
3. Reich, P.B., *The world-wide 'fast–slow' plant economics spectrum: a traits manifesto.* Journal of Ecology, 2014. **102**(2): p. 275-301.
4. Donovan, L.A., et al., *The evolution of the worldwide leaf economics spectrum.* Trends in Ecology & Evolution, 2011. **26**(2): p. 88-95.
5. Díaz, S., et al., *The global spectrum of plant form and function.* Nature, 2016. **529**(7585): p. 167-171.
6. Gornish, E.S. and C.M. Prather, *Foliar functional traits that predict plant biomass response to warming.* Journal of Vegetation Science, 2014. **25**(4): p. 919-927.
7. Anderegg, L.D.L., et al., *Within-species patterns challenge our understanding of the leaf economics spectrum.* Ecology Letters, 2018. **21**(5): p. 734-744.
8. Messier, J., et al., *Trait variation and integration across scales: is the leaf economic spectrum present at local scales?* Ecography, 2017. **40**: p. 685-697.

9. Edwards, E.J., et al., *Leaf life span and the leaf economic spectrum in the context of whole plant architecture.* Journal of Ecology, 2014. **102**(2): p. 328-336.
10. Lynch, M. and B. Walsh, *Genetics and analysis of quantitative traits*. 1998, Sunderland, MA: Sinauer.
11. Lande, R. and S.J. Arnold, *The measurement of selection on correlated characters.* Evolution, 1983: p. 1210-1226.
12. Svensson, E.I., et al., *Correlational selection in the age of genomics.* Nature Ecology & Evolution, 2021. **5**: p. 562-573.
13. Walsh, B. and M.W. Blows, *Abundant genetic variation + strong selection = multivariate genetic constraints: a geometric view of adaptation.* Annual Review of Ecology, Evolution, and Systematics, 2009. **40**(1): p. 41-59.
14. Heckman, R.W., et al., *Changes in leaf economic trait relationships across a precipitation gradient are related to differential gene expression in a C_4 perennial grass.* New Phytologist, 2025. **246**(4): p. 1583–1596.
15. Mackay, T.F.C., *The genetic architecture of quantitative traits.* Annual Review of Genetics, 2001. **35**(1): p. 303-339.
16. Sinervo, B. and E. Svensson, *Correlational selection and the evolution of genomic architecture.* Heredity, 2002. **89**(5): p. 329-338.
17. Guilherme Pereira, C. and D.L. Des Marais, *The genetic basis of plant functional traits and the evolution of plant-environment interactions.* International Journal of Plant Sciences, 2020. **181**(1): p. 56-74.
18. Heckman, R.W., et al., *Physiological responses of C_4 perennial bioenergy grasses to climate change: causes, consequences, and constraints.* Annual Review of Plant Biology, 2024. **75**: p. 737-769.
19. Mooney, H.A., *The carbon balance of plants.* Annual Review of Ecology and Systematics, 1972. **3**: p. 315-346.
20. Mason, C.M. and L.A. Donovan, *Evolution of the leaf economics spectrum in herbs: Evidence from environmental divergences in leaf physiology across Helianthus (Asteraceae).* Evolution, 2015. **69**(10): p. 2705-2720.
21. Grady, K.C., et al., *Conservative leaf economic traits correlate with fast growth of genotypes of a foundation riparian species near the thermal maximum extent of its geographic range.* Functional Ecology, 2013. **27**(2): p. 428-438.
22. Ahrens, C.W., P.D. Rymer, and D.T. Tissue, *Intra-specific trait variation remains hidden in the environment.* New Phytologist, 2021. **229**(3): p. 1183-1185.
23. Swenson, N.G., et al., *A reframing of trait–demographic rate analyses for ecology and evolutionary biology.* International Journal of Plant Sciences, 2020. **181**(1): p. 33-43.
24. Pérez-Harguindeguy, N., et al., *New handbook for standardised measurement of plant functional traits worldwide.* Australian Journal of Botany, 2013. **61**(3): p. 167-234.
25. Aspinwall, M.J., et al., *Genotypic variation in traits linked to climate and aboveground productivity in a widespread C_4 grass: evidence for a functional trait syndrome.* New Phytologist, 2013. **199**(4): p. 966-980.
26. Mauricio, R., *Mapping quantitative trait loci in plants: uses and caveats for evolutionary biology.* Nature Reviews Genetics, 2001. **2**(5): p. 370-381.
27. Anderson, J.T. and T. Mitchell-Olds, *Ecological genetics and genomics of plant defences: evidence and approaches.* Functional Ecology, 2011. **25**(2): p. 312-324.

28. Caruso, C.M., C.M. Mason, and J.S. Medeiros, *The evolution of functional traits in plants: is the giant still sleeping?* International Journal of Plant Sciences, 2020. **181**(1): p. 1-8.
29. Brodie, E.D., A.J. Moore, and F.J. Janzen, *Visualizing and quantifying natural selection.* Trends in Ecology & Evolution, 1995. **10**(8): p. 313-318.
30. Boehm, F.J., et al., *Testing pleiotropy vs. separate QTL in multiparental populations.* G3 Genes|Genomes|Genetics, 2019. **9**(7): p. 2317-2324.
31. Gromko, M.H., *Unpredictability of correlated response to selection: pleiotropy and sampling interact.* Evolution, 1995. **49**(4): p. 685-693.
32. Rausher, M.D., *The measurement of selection on quantitative traits: biases due to environmental covariances between traits and fitness.* Evolution, 1992. **46**(3): p. 616-626.
33. Agrawal, A.A., *A scale-dependent framework for trade-offs, syndromes, and specialization in organismal biology.* Ecology, 2020. **101**(2): p. e02924.
34. Chenoweth, S.F., Howard D. Rundle, and Mark W. Blows, *The contribution of selection and genetic constraints to phenotypic divergence.* The American Naturalist, 2010. **175**(2): p. 186-196.
35. Hanemian, M., et al., *Natural variation at FLM splicing has pleiotropic effects modulating ecological strategies in Arabidopsis thaliana.* Nature Communications, 2020. **11**(1): p. 4140.
36. Vasseur, F., et al., *A common genetic basis to the origin of the leaf economics spectrum and metabolic scaling allometry.* Ecology Letters, 2012. **15**(10): p. 1149-1157.
37. Milano, E.R., D.B. Lowry, and T.E. Juenger, *The genetic basis of upland/lowland ecotype divergence in switchgrass (Panicum virgatum).* G3 Genes|Genomes|Genetics, 2016. **6**(11): p. 3561-3570.
38. Sartori, K., et al., *Leaf economics and slow-fast adaptation across the geographic range of Arabidopsis thaliana.* Scientific Reports, 2019. **9**(1): p. 10758.
39. Durant, P.C., et al., *Genetically correlated leaf tensile and morphological traits are driven by growing season length in a widespread perennial grass.* American Journal of Botany, 2024. **111**(5): p. e16349.
40. Heckman, R.W., et al., *Plant biomass, not plant economics traits, determines responses of soil CO_2 efflux to precipitation in the C_4 grass Panicum virgatum.* Journal of Ecology, 2020. **108**(5): p. 2095-2106.
41. Ricketts, M.P., et al., *Local adaptation of switchgrass drives trait relations to yield and differential responses to climate and soil environments.* GCB Bioenergy, 2023. **15**(5): p. 680-696.
42. Lowry, D.B., et al., *Adaptations between ecotypes and along environmental gradients in Panicum virgatum.* American Naturalist, 2014. **183**(5): p. 682-92.
43. Lovell, J.T., et al., *Genomic mechanisms of climate adaptation in polyploid bioenergy switchgrass.* Nature, 2021. **590**(7846): p. 438-444.
44. Chen, W., et al., *The genetic basis of the root economics spectrum in a perennial grass.* Proceedings of the National Academy of Sciences, 2021. **118**(47): p. e2107541118.
45. Lowry, D.B., et al., *QTL × environment interactions underlie adaptive divergence in switchgrass across a large latitudinal gradient.* Proceedings of the National Academy of Sciences, 2019. **116**(26): p. 12933.

46. Meyer, E., et al., *Integrating transcriptional, metabolomic, and physiological responses to drought stress and recovery in switchgrass (Panicum virgatum L.).* BMC Genomics, 2014. **15**: p. 527.
47. Arnold, S.J., *Morphology, performance and fitness.* American Zoologist, 1983. **23**(2): p. 347-361.
48. Franklin, O.D. and M.B. Morrissey, *Inference of selection gradients using performance measures as fitness proxies.* Methods in Ecology and Evolution, 2017. **8**(6): p. 663-677.
49. Palik, D.J., et al., *Relative performance of non-local cultivars and local, wild populations of Switchgrass (Panicum virgatum) in competition experiments.* PLOS ONE, 2016. **11**(4): p. e0154444.
50. Caruso, C.M., H. Maherali, and R.A. Martin, *A meta-analysis of natural selection on plant functional traits.* International Journal of Plant Sciences, 2020. **181**(1): p. 44-55.
51. Warton, D.I., et al., *smatr 3– an R package for estimation and inference about allometric lines.* Methods in Ecology and Evolution, 2012. **3**(2): p. 257-259.
52. Warton, D.I., et al., *Bivariate line-fitting methods for allometry.* Biological Reviews, 2006. **81**(2): p. 259-291.
53. Covarrubias-Pazaran, G., *Genome-assisted prediction of quantitative traits using the R package sommer.* PLOS ONE, 2016. **11**(6): p. e0156744.
54. Wilson, A.J., et al., *An ecologist's guide to the animal model.* Journal of Animal Ecology, 2010. **79**(1): p. 13-26.
55. Hill, W.G., *On estimation of genetic variance within families using genome-wide identity-by-descent sharing.* Genetics Selection Evolution, 2013. **45**(1): p. 32.
56. Broman, K.W., et al., *R/qtl2: Software for Mapping Quantitative Trait Loci with High-Dimensional Data and Multiparent Populations.* Genetics, 2019. **211**(2): p. 495-502.
57. Lovell, J., et al., *Switchgrass v5 4-way (AP13 x DAC, WBC x VS16) genetic map*. 2020: Dryad https://datadryad.org/stash/dataset/doi:10.5061/dryad.ghx3ffbjv.
58. Broman, K.W., et al., *R/qtl: QTL mapping in experimental crosses.* Bioinformatics, 2003. **19**(7): p. 889-890.
59. Pinheiro, J., et al., *nlme: linear and nonlinear mixed effects models. R package version 3.1–127.* 2016.
60. Stinchcombe, J.R., et al., *Estimating nonlinear selection gradients using quadratic regression coefficients: double or nothing?* Evolution, 2008. **62**(9): p. 2435-2440.

Figures and Tables

Figure 1. Relationship between **A)** leaf mass-based nitrogen concentration (N_{MASS}; %) and leaf mass per area (LMA; g m^{-2}); **B)** leaf mass-based photosynthetic rate (A_{MASS}; μmol C g^{-1} s^{-1}) and LMA; **C)** A_{MASS} and N_{MASS}, calculated using standardized major axis regression. Black dots are *P. virgatum* F_2 individuals; blue triangles are grandparental (F_0) line means (not included in SMA line fit). Inset plots show the location of *P. virgatum* F_2 individuals (black dots) relative to the worldwide leaf economics spectrum (grey dots; from Wright et al. 2004) on a $\log_{10}$–$\log_{10}$ scale.

Figure 2. A) Location of QTL for three leaf economics traits, LMA, N_{MASS}, and A_{MASS}. Point estimates are the location of highest LOD score and confidence intervals are the region within a 1.5 LOD drop. **B)** Effects of genotype on leaf economics traits at three colocalized QTL markers (i.e., markers with overlapping confidence intervals) calculated using ordinary least squares regression. Genotypes at each QTL are a consequence of recombination in the experimental cross, resulting in four possible combinations of alleles. In each panel, Lowland1 and Lowland2 denote alleles inherited from genotypes AP13 and WBC, respectively; Upland1 and Upland2 denote alleles inherited from genotypes DAC and VS16, respectively. Error bars represent 95% confidence intervals; shared letters indicate no significant difference between genotypes. For all colocalized QTL pairs, genotype effects are in a consistent direction (i.e., each genotype exhibits conservative or acquisitive values of both traits) and are consistent with statistical pleiotropy. See Figure 1 legend for units and abbreviations.

Figure 3. Effects of standardized LMA and N_{MASS} (mean-centered and variance-standardized) on relative biomass (mean-standardized) averaged across genotypes replicated at three sites. Model-derived quadratic parameter estimates are doubled. See Figure 1 legend for units and abbreviations.

Figure 4. Effects of standardized LMA and N_{MASS} (mean-centered and variance-standardized) on relative biomass (mean-standardized) separately at three sites. **A)** Linear selection on N_{MASS} at the southernmost site in Texas, **B)** Correlational selection on LMA and N_{MASS} at the mid-latitude site in Missouri and C) at the northernmost site in Michigan. In panels **B** and **C**, model-derived quadratic parameter estimates are doubled. See Fig. 1 legend for units and abbreviations.

Figure 1

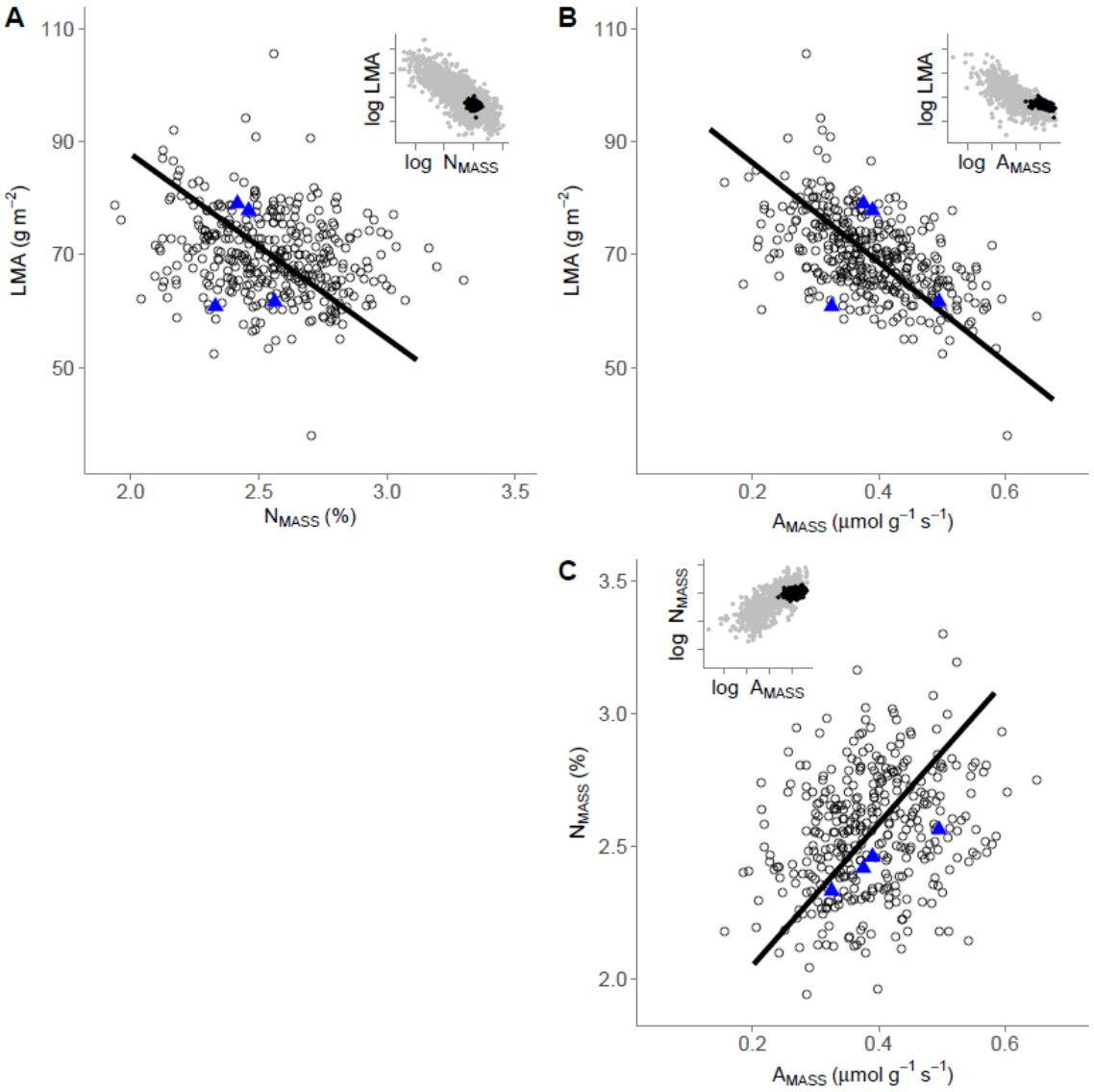
A
B
C
LMA (g m^{-2})
N_{MASS} (%)
A_{MASS} (µmol g^{-1} s^{-1})
log LMA
log N_{MASS}
log A_{MASS}
110
90
70
50
2.0
2.5
3.0
3.5
0.2
0.4
0.6

Figure 2

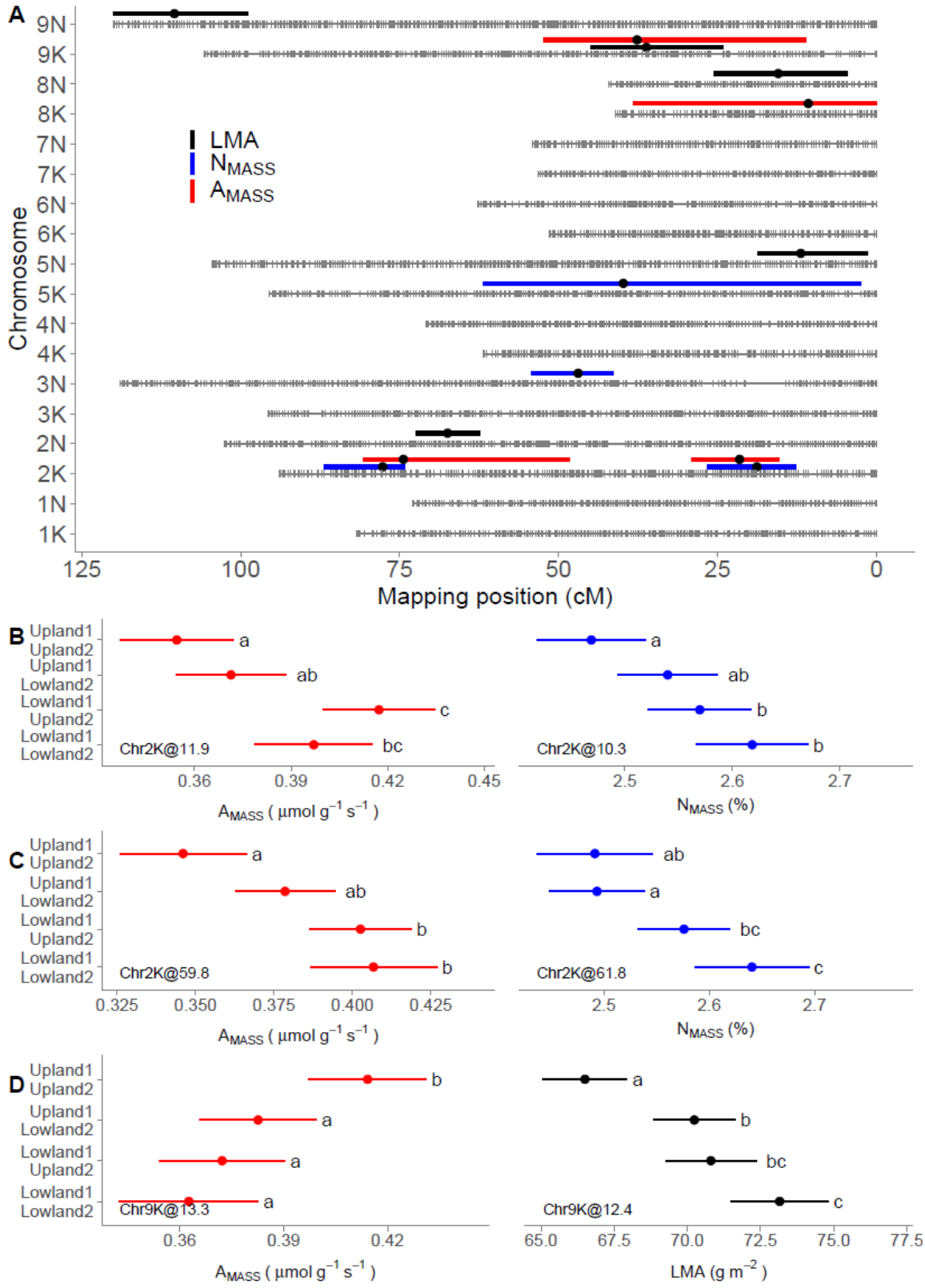
A
Chromosome
9N
9K
8N
8K
7N
7K
6N
6K
5N
5K
4N
4K
3N
3K
2N
2K
1N
1K
LMA
NMASS
AMASS
125
100
75
50
25
0
Mapping position (cM)
B
Upland1
Upland2
Upland1
Lowland2
Lowland1
Upland2
Lowland1
Lowland2
a
ab
c
bc
Chr2K@11.9
0.36
0.39
0.42
0.45
AMASS (µmol g−1 s−1)
a
ab
b
b
Chr2K@10.3
2.5
2.6
2.7
NMASS (%)
C
a
ab
b
b
Chr2K@59.8
0.325
0.350
0.375
0.400
0.425
AMASS (µmol g−1 s−1)
ab
a
bc
c
Chr2K@61.8
2.5
2.6
2.7
NMASS (%)
D
b
a
a
a
Chr9K@13.3
0.36
0.39
0.42
AMASS (µmol g−1 s−1)
a
b
bc
c
Chr9K@12.4
65.0
67.5
70.0
72.5
75.0
77.5
LMA (g m−2)

Figure 3

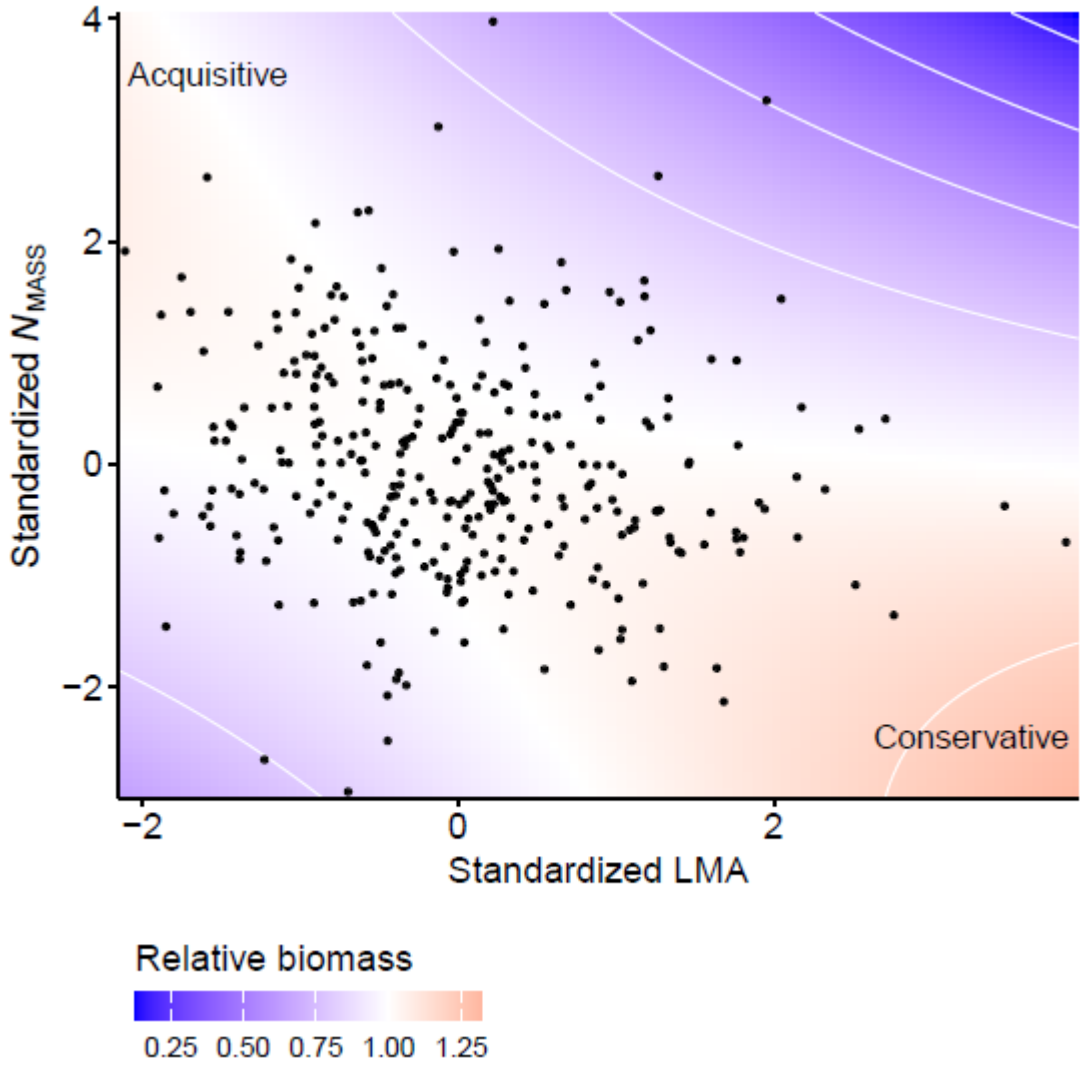
Acquisitive
Conservative
Standardized N_{MASS}
Standardized LMA
4
2
0
−2
−2
0
2
Relative biomass
0.25 0.50 0.75 1.00 1.25

Figure 4

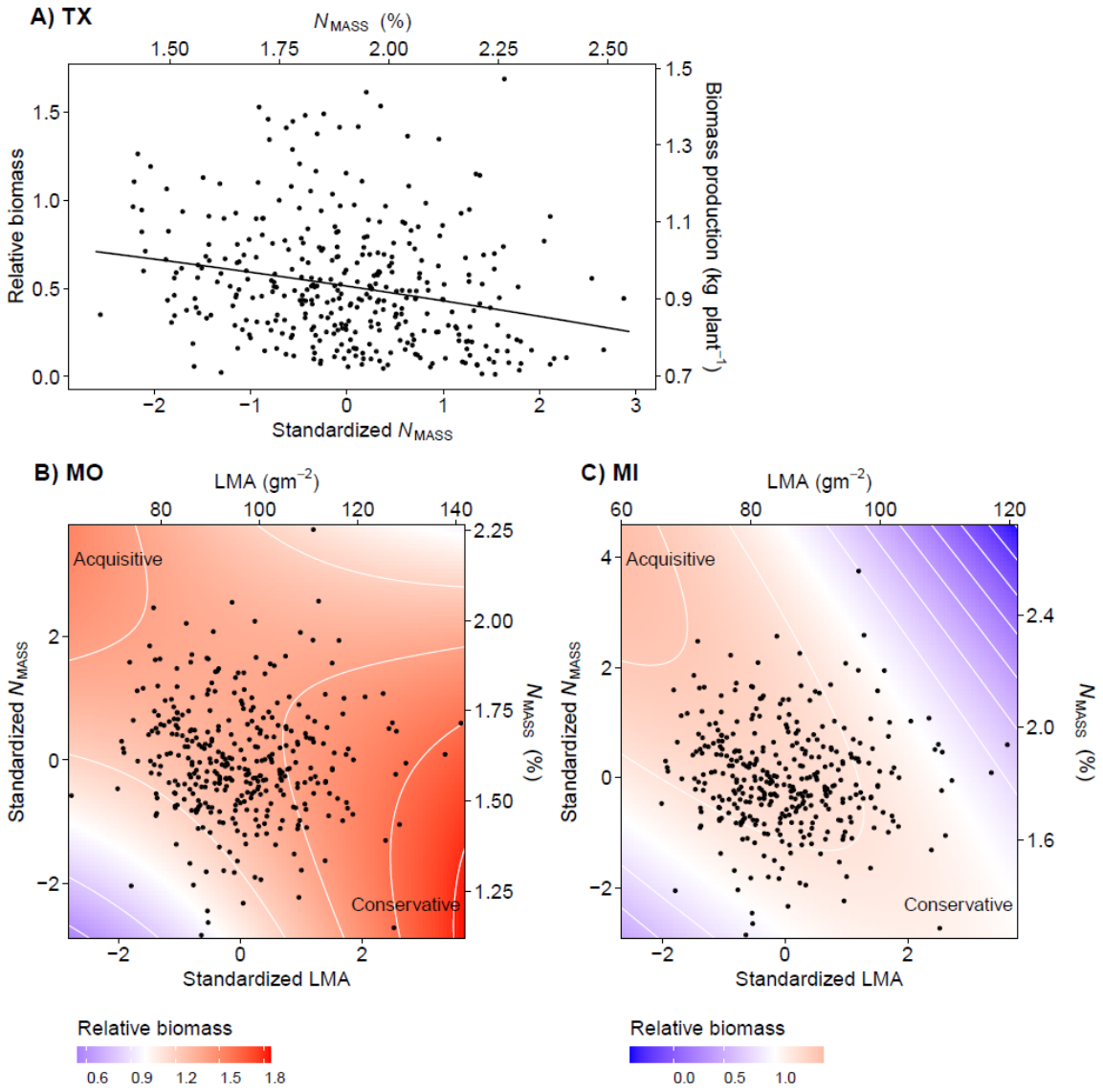
A) TX
N_{MASS} (%)
1.50
1.75
2.00
2.25
2.50
Relative biomass
Biomass production (kg plant^{-1})
Standardized N_{MASS}
B) MO
LMA (gm^{-2})
Acquisitive
Conservative
Standardized N_{MASS}
N_{MASS} (%)
Standardized LMA
Relative biomass
0.6 0.9 1.2 1.5 1.8
C) MI
LMA (gm^{-2})
Acquisitive
Conservative
Standardized N_{MASS}
N_{MASS} (%)
Standardized LMA
Relative biomass
0.0 0.5 1.0

Table 1. Genetic basis of three leaf economics traits. H^2 is broad-sense heritability [V_G / (V_G + V_E)] ± standard error; variance explained by QTL is calculated from a multiple-QTL model using all identified putative QTL as predictors of each trait; proportion of heritable variation explained by QTL is the ratio of variance explained by QTL to H^2. LMA is leaf mass per area; A_{MASS} is mass-based leaf photosynthetic rate; N_{MASS} is mass-based leaf nitrogen concentration.

	H^2	Variance explained by QTL	Proportion of heritable variation explained by QTL
LMA	0.51 ± 0.07	0.35	0.69
A_{MASS}	0.26 ± 0.08	0.15	0.58
N_{MASS}	0.46 ± 0.08	0.24	0.52

Table 2. Significant QTL markers for each leaf economics trait detected at a LOD threshold of α = 0.15. *P* values are based on *F* tests calculated by dropping one QTL at a time from a multiple-QTL model that included all putative QTL for each trait. LMA is leaf mass per area; A_{MASS} is mass-based leaf photosynthetic rate; N_{MASS} is mass-based leaf nitrogen concentration.

Trait	Marker position (Mb)	Mapping position (cM)	LOD	*P*
LMA	Chr2N@56.1	67.46	3.972	< 0.001
	Chr5N@4.9	11.92	7.814	< 0.001
	Chr8N@13.7	15.46	3.873	< 0.001
	Chr9K@12.4	36.20	10.359	< 0.001
	Chr9N@79.4	110.41	4.173	< 0.001
A_{MASS}	Chr2K@11.9	21.55	6.079	< 0.001
	Chr2K@59.8	74.41	4.580	0.017
	Chr8K@11.3	10.75	4.771	< 0.001
	Chr9K@13.3	37.68	3.896	0.002
N_{MASS}	Chr2K@10.3	18.83	4.164	< 0.001
	Chr2K@61.8	77.66	5.601	< 0.001
	Chr3N@16.5	46.93	8.592	< 0.001
	Chr5K@21.5	39.82	3.929	< 0.001

Table 3. Genetic correlations between leaf economics traits with standard errors. LMA is leaf mass per area; A_{MASS} is mass-based leaf photosynthetic rate; N_{MASS} is mass-based leaf nitrogen concentration.

	LMA	A_{MASS}	N_{MASS}
LMA	---		
A_{MASS}	**-0.76** (0.12)	---	
N_{MASS}	-0.16 (0.17)	0.26 (0.21)	---

Table 4. Table showing standardized effects of two standardized leaf economics traits on plant relative biomass. In **A**, all traits were averaged within genotypes across sites; In **B**–**D**, estimates come from models fit separately to each site. In each column, the first value is the parameter estimate from selection gradient model and standard errors of these estimates are in parentheses. Linear selection coefficients were estimated from models fit to the linear terms only (i.e., main effects). Non-linear selection coefficients (quadratic and interaction terms) were estimated from models that included linear and non-linear terms. All quadratic term estimates are doubled. LMA is leaf mass per area; N_{MASS} is mass-based leaf nitrogen concentration.

	Phenotypic selection gradients			
Parameter	A) Global	B) TX	C) MO	D) MI
LMA	0.005 (0.017)	0.004 (0.018)	0.070 (0.025)	-0.038 (0.022)
N_{MASS}	-0.012 (0.017)	-0.081 (0.018)	0.039 (0.027)	0.026 (0.025)
LMA^2	-0.006 (0.023)	0.023 (0.023)	0.010 (0.034)	-0.059 (0.027)
N_{MASS}^2	-0.029 (0.020)	-0.005 (0.027)	-0.040 (0.033)	-0.043 (0.026)
LMA × N_{MASS}	-0.037 (0.017)	-0.001 (0.017)	-0.043 (0.026)	-0.051 (0.024)